

Mapping the extended TeV source HESS J1857+026 down to Fermi-LAT energies with the MAGIC telescopes

STEFAN KLEPSE¹, JULIAN KRAUSE², MICHELE DORO³ FOR THE MAGIC COLLABORATION

¹*IFAE, Edifici Cn., Campus UAB, E-08193 Bellaterra, Spain*

²*Max-Planck-Institut für Physik, D-80805 München, Germany*

³*Universitat Autònoma de Barcelona, E-08193 Bellaterra, Spain*

klepser@ifae.es

Abstract: HESS J1857+026 is an extended TeV gamma-ray source discovered by H.E.S.S. very close to the Galactic plane. Located in the vicinity of the pulsar PSR J1856+0245, the source represents a pulsar wind nebula (PWN) candidate. In Fermi-LAT data, 7 photons above 100 GeV were associated to it as VHE J1857+0252 by Neronov and Semikoz (2010), while in the previous MeV-GeV catalogs no associated source was reported yet. MAGIC was upgraded to a stereoscopic Cherenkov telescope system in 2009, which substantially improved its performance with respect to extended objects. We observed HESS J1857+026 in 2010 and analysed 29 hours of good quality stereoscopic data, yielding a highly significant detection. We present an energy spectrum from 100 GeV to 10 TeV and skymaps for two different energy regimes. The spectrum does not show any indication for an inverse Compton turnover, while we find an intrinsic extension of $\sigma = 0.22 \pm 0.02_{\text{stat}} \pm 0.02_{\text{sys}}$ in the energy range of 200 – 1000 GeV. We discuss the possible PWN nature of the source and the performance of MAGIC with respect to extended sources.

Keywords: MAGIC, pulsar wind nebulae, HESS J1857+026, very-high energy gamma-rays

1 Introduction

The H.E.S.S. collaboration reported a series of unidentified very high energy (VHE, > 100 GeV) gamma-ray objects found in their survey of the Galactic plane [1]. Among them is the extended source HESS J1857+026, which is situated at only 0.056° from the Galactic plane and was estimated to have a flux of about 16 % c.u. (Crab units). From 21 h of data and 223 excess events, H.E.S.S. derived a detection significance of 8.7σ and a spectrum was extracted from 800 GeV to 45 TeV compatible with a power law of index 2.39 ± 0.08 . The extension was slightly beyond the H.E.S.S. resolution, $(0.11 \pm 0.08)^\circ \times (0.08 \pm 0.03)^\circ$, and a significant tail-like structure on the northern edge of the object was denoted. The VERITAS team confirmed this detection in 2009 from 13 h of data without providing more details [2].

In 2008, after the H.E.S.S. detection, a Vela-like pulsar PSR J1856+0245 was found in close vicinity of HESS J1857+026 [3]. It has a spin period of 81 ms, a characteristic age of 21 kyr, and a spin-down luminosity of 4.6×10^{36} ergs s^{-1} . The authors of [3] suggest that the pulsar might be powering a pulsar wind nebula (PWN) that produces VHE gamma rays through inverse Compton scattering. The distance to the pulsar was found to be about 9 kpc, but could only be estimated from the dispersion measure, and is therefore uncertain within a factor of

2-3. This large distance leads to the high spin-down flux, which energetically makes it a viable candidate to feed the VHE object. A faint X-ray emission detected by ASCA in the same area supported this idea (also [3]).

On the MeV-GeV gamma-ray side, no source was reported in GeV neither by the EGRET team nor in the first Fermi/LAT catalog. Only in late 2010, Neronov and Semikoz [4] stated a significant detection of 7 clustered photons above 100 GeV, and a corresponding flux of $(20.3 \pm 7.4) \times 10^{-10}$ cm $^{-2}$ s $^{-1}$ TeV $^{-1}$, normalized at 100 GeV. Even more recently, this detection was confirmed by the Fermi/LAT team, stating a fitted position compatible with that found by H.E.S.S. [5]. An indication for pulsation was not found, which is conform with the idea that the gamma rays might emerge from inverse Compton scattering of diffuse electrons in a PWN. Besides that, no extension was found, but no quantitative limit on the extension was given. On the same conference, HESS J1857+026 appeared in a list of Fermi sources above 10 GeV, including an integral flux above 10 GeV, and an index of 1.30 ± 0.28 , indicating a hardening at lower energies.

A way to prove the PWN nature of HESS J1857+026 is to analyse the spectrum and the morphology evolution with energy. Inverse Compton scattering in PWN is expected to produce a curved spectrum with a peak that in many cases lies in the TeV energy range (see e.g. [7] for a review). Its position depends however on many factors and may be, as

in case of the Crab Nebula, at energies as low as some tens of GeV. In the H.E.S.S. spectrum of HESS J1857+026, no hint for a turnover can be seen, indicating the peak energy must be at least below 800 GeV. At the same time, low-energetic electrons have a longer mean free path length, and might diffuse farther away from the pulsar, so an extending morphology at lower energies might give another hint towards a PWN scenario.

The two MAGIC telescopes [8], situated on the island of La Palma (28.8° N, 17.8° W, 2220 m a.s.l.), use the Imaging Atmospheric Cherenkov Technique (IACT) to detect gamma rays above a threshold as low as 75 – 80 GeV in standard trigger mode¹. Since it started operating in stereoscopic mode in summer 2009, its background suppression was substantially reduced and a sensitivity² of 0.8 % c.u. above 250 GeV could be achieved [10]. Also, the MAGIC-II camera comprises a bigger trigger area, which improved the off-axis performance of MAGIC, a feature that is crucial for new source discoveries and extended sources.

2 Data set

We observed HESS J1857+026 on 33 days between 2010 July 11 and 2010 October 10, obtaining 29 h of good-quality data (effective on-time after all cuts) at zenith angles between 25° and 36°. The data was taken in wobble mode, pointing the telescopes at 4 different pairs of pointing directions symmetric to the source position, to achieve a better flatness of exposure. Two of these pairs were chosen to be at 0.4° distance from the source, embracing it like a cross, and two more at 0.5°, also like a cross. This setup allows a large variety of cross-checks and performance studies between different wobble pairs.

3 Analysis methods and performance

The analysis of the data was done with the MARS analysis framework [9], including the latest standard routines for stereoscopic analysis, whose performance is also presented on this conference [10]. Besides the abovementioned sensitivity and analysis threshold, it provides an angular resolution of about 0.055° (0.075°) at 1 TeV (250 GeV). The energy estimator is calculated from the brightness of the shower image, its reconstructed impact parameter and the zenith angle, using look-up tables. For the gamma/hadron separation and gamma direction estimation we use the random forest (RF) technique [11]. We tested both our standard random forests (*point-source* RF), which are trained with gamma rays simulated as a point-source MonteCarlo (*point-source* MC), and a random forest trained with diffusely generated gammas (*diffuse* RF/MC).

3.1 Skymapping

For the skymaps, a three-step algorithm is applied as reported in some detail also on this conference [12]. This

algorithm models the background directly from the data and in bins of azimuth, properly taking into account azimuthal dependencies of the off-axis sensitivity. To facilitate the interpretation of structures, the events are folded (smeared) with a Gaussian kernel in order to achieve a point spread function with a Gaussian shape and a total width of $\sigma_{\text{tot}}^2 = \sigma_{\text{smear}}^2 + \sigma_{\text{analysis}}^2$. The width of the analysis-intrinsic resolution, σ_{analysis} , is determined from MC, and cross-checked with Crab Nebula data. In the two skymaps presented here, the smearing kernel is adjusted such that $\sigma_{\text{tot}} = 0.11^\circ$. With our intrinsic resolution of 0.055° – 0.075°, a finer smearing would be possible to see more details, but the noise that comes with the higher trial factor also distorts the image, so the σ_{tot} we chose is a compromise between low noise and high resolution.

3.2 Spectral Analysis

The spectrum was calculated for a circular area with a radius of 0.4°, centered on our fitted position. To estimate the average effective area, a MC dataset was used with gammas simulated on a ring around the observation center, with inner and outer radii of 0.25° and 0.65°. This is done to take the variations of acceptance across the area of the source into account. Besides the tests described in the next paragraph, we cross-checked the spectrum normalizing the background estimation by event numbers in off-source areas, or by effective on-time, and using 4 different unfolding algorithms [13].

3.3 Performance with Extended Sources

We conducted several tests to evaluate the performance of our analysis tools with respect to extended sources. The main conclusions we could draw are:

- The significance, skymap and spectral analyses done with **point-source and diffuse RFs** agree well within statistical errors unless a very tight cut in the *hadronness* parameter is applied. A tight hadronness cut is equivalent to a high dependency on MC, so this discrepancy is conform with what can be expected from the method.
- The spectrum shown in this contribution can be reproduced within systematic errors even using our standard 0.4°-offset **point-source MC instead of the ring-like MC** described above.
- Since the source peak is slightly misplaced with respect to the center of observations, we have considerable geometric exposure inhomogeneities. We therefore tried 2 different ways of **deriving a background estimate**: One is to simply use the background data

1. defined as the peak of the true energy distribution after all cuts and at low zenith angles

2. defined as source strength in c.u. needed to achieve $N_{\text{ex}}/\sqrt{N_{\text{bkg}}} = 5$ in 50 h effective on-time.

from the anti-source position within each wobble sub-set, the other one is taking it from the corresponding *wobble partner* data set, extracting it at the same relative focal plane coordinates as the source position in the On-data. The latter should be subject to less systematic errors, but both methods again turn out to agree within systematic errors.

Concluding, we see that the analysis scheme we opted for is very robust against the possible variations of it. The results we present here are finally derived using the diffuse RFs and MC, and the wobble partner background estimation.

4 Results

We detected > 3000 gamma-like excess events above 100 GeV, providing us with a detection significance exceeding 12σ . From these events, we calculated two skymaps for the energy range of 200 GeV – 1 TeV, and > 1 TeV (estimated energies). The median true energies of the gamma rays in these maps were estimated from MC to be 370 GeV and 1.8 TeV, respectively. The results are shown in Figure 1.

In the high energy map, there are two significant structures found, roughly confirming what the H.E.S.S. team found. The energy regime in their map is probably similar, although their higher effective area at high energies might lead to a higher median energy.

The low energy skymap looks very different: There is only one structure, roughly centered at the position of HESS J1857+026. We fit the emission center to be located at R.A. = $(18.953 \pm 0.002_{\text{stat}} \pm 0.002_{\text{sys}})$ h and Decl. = $(2.70 \pm 0.02_{\text{stat}} \pm 0.03_{\text{sys}})^{\circ}$, compatible within errors with the positions determined by H.E.S.S. and Fermi/LAT.

In this low energy skymap, we find the source to be clearly extended beyond the $\sigma_{\text{tot}} = 0.11^{\circ}$ implied by our PSF and smearing. The source-intrinsic extension we derive after subtraction of our total PSF in this energy range is $0.22^{\circ} \pm 0.02^{\circ}_{\text{stat}} \pm 0.02^{\circ}_{\text{sys}}$. This extension was fitted assuming a two-dimensional Gaussian shape with or without circular symmetry (the eccentricity is not significantly different from 0). It was also cross-checked using different random forest matrices, as described in the previous section.

The energy spectrum we derived is shown in Figure 2. It spans over two orders of magnitude and is compatible with a power law of index $2.27 \pm 0.08_{\text{stat}} \pm 0.1_{\text{sys}}$ and flux constant at 1 TeV of $(4.7 \pm 0.6_{\text{stat}} \pm 1.4_{\text{sys}}) \times 10^{-12} \text{ TeV}^{-1} \text{ cm}^{-2} \text{ s}^{-1}$. This is compatible with the parameters and spectral points found by H.E.S.S., although maybe in slight disagreement with the Fermi/LAT estimate given in [4]. The spectrum at and below 100 GeV is still being investigated for systematic effects and will be published in a forthcoming paper.

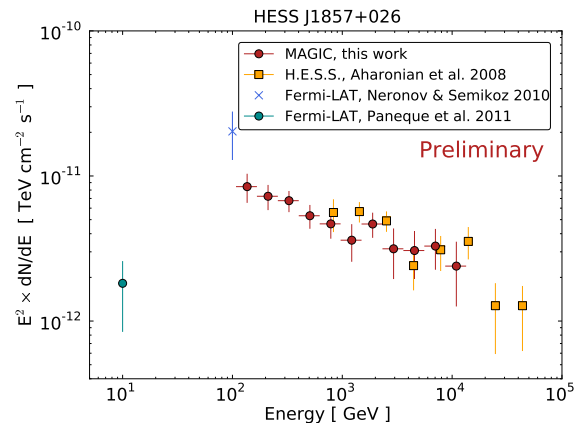


Figure 2: Spectral energy distributions of HESS J1857+026 measured by MAGIC, H.E.S.S. [1] and Fermi/LAT [4, 6]. The MAGIC data is unfolded to correct for migration and biasing effects, therefore the errors are not independent.

5 Discussion and Outlook

The extension we find in the energy regime of 200 GeV – 1 TeV is significantly higher than the extension reported by H.E.S.S. at higher energies. This might support the idea that low-energetic electrons from the PWN create this radiation after diffusing far away from the pulsar. However, this reasoning only holds if the northern tail of the source is not regarded part of the PWN, since it does not seem to have a low-energy counterpart, implying a harder spectrum despite the larger distance to the pulsar. The extension we see for the PWN at high energies is still under investigation, but seems to be smaller than at low energies (though still larger than the one reported by H.E.S.S., which might be attributed to the possibly higher median true energy of the H.E.S.S. detection and is not necessarily a conflict).

The spectrum we find above 100 GeV shows no features nor a significant curvature. This is not strongly contradicting a possible PWN scenario, but does not provide the evidence which a curved (IC motivated) shape would have constituted. Adding the low integral flux and photon index reported in [6] (see Figure 2), and the fact that no source was previously found in the MeV-GeV domain, allows for the conclusion that the spectrum has a very flat shape over 2-3 orders of magnitude, and a relatively hard turnover at energies close to 100 GeV. Compared to the well-studied PWN HESS J1825-137 [14, 15], which is located at about half the distance of HESS J1857+026, but with a very similar pulsar age and period, we find the spectral parameters and features are strikingly similar, except the TeV spectrum is more clearly curved in HESS J1825-137.

Concerning the northern tail of the emission, it seems that it must be either a different object altogether, or a different mechanism that is at work. If it were connected to the main emission spot in some way, its distance to the pulsar

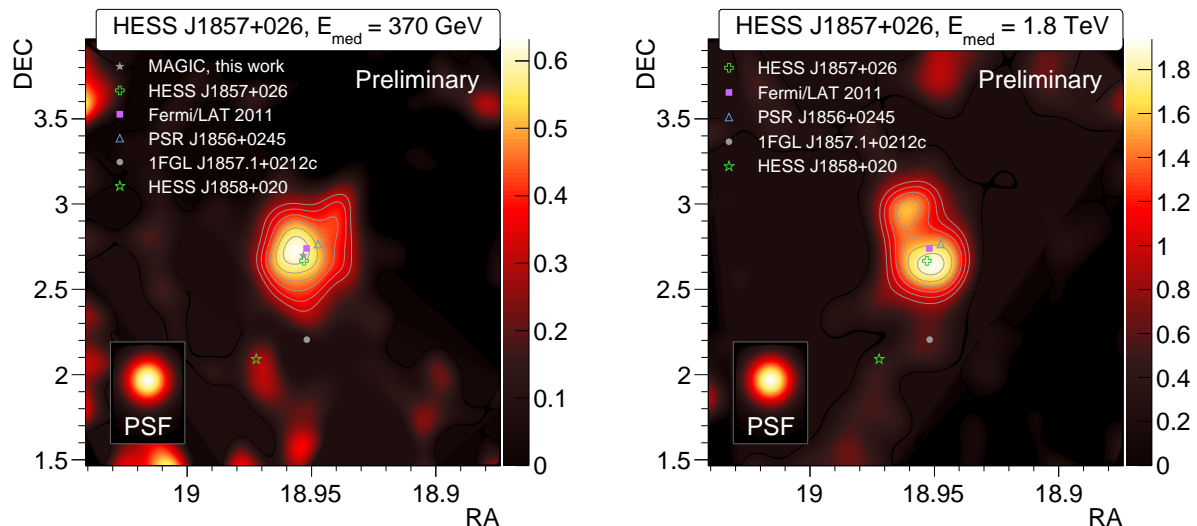


Figure 1: MAGIC "relative flux" map for events with $200 \text{ GeV} < E_{\text{est}} < 1 \text{ TeV}$ and $E_{\text{est}} > 1 \text{ TeV}$. The indicated median energies are calculated from a MC that is reweighted to resemble the spectrum of the source. The relative flux is calculated after smearing as $N_{\text{ex}}/N_{\text{bkg}, < 0.1^\circ}$ and is roughly proportional to the actual gamma flux. Overlaid are TS value contours in steps of 1, starting at 3. They roughly correspond to Gaussian significances (for more information about the relative flux and our TS, see [12]). The fact that we do not significantly detect HESS J1858+020 might be attributed to the MAGIC exposure at this distance to the observed sky positions, and will not be discussed in this paper.

would be $\sim 50 \text{ pc} \times (d/9 \text{ kpc})$, which does not exclude in general an association as for instance through interactions of an expanding SNR shell from the same supernova event. To possibly shed more light on the nature of this northern tail of the source, we are presently working on a refined analysis, trying to extract spatially resolved spectra, and more differential skymaps. Also, we will reanalyse the data at and below 100 GeV to provide more information about the position and shape of the spectral turnover. Besides that, we have to understand whether or not there is a conflict with the Fermi/LAT analysis in [5], which claimed no extension at lower energies and might provide a quantitative extension limit in the near future.

Concluding, we exploited the newly improved sensitivity of MAGIC to extended sources to study the PWN HESS J1857+026, and present a very wide, featureless energy spectrum and two skymaps. We find that the northern, tail-like structure shown by H.E.S.S. does not have a counterpart at lower energies. Instead, only a more extended object can be seen at the position compatible with the coordinates of HESS J1857+026. We also find that the morphology and overall spectral shape of the main emission zone supports the concept of a PWN nature of HESS J1857+026, which therewith exhibits several similarities with the known PWN HESS J1825-137. However, the wide-range, flat TeV spectrum and the apparently different spectral behaviour of the northern tail of the source might still indicate a more complex scenario for this object. A more detailed analysis of the MAGIC data, to be published in a forthcoming paper, will provide a detailed spectral and morphological study that might deliver more insight in the nature of HESS J1857+026.

References

- [1] Aharonian, F. et al., *A&A*, 2008, **477**(353)
- [2] Ong, R.A. et al., Proc. 31st ICRC (Łódź), 2009 (arXiv:0912.5355)
- [3] Hessels, J.W. et al., *ApJ*, 2008, **682**(L41)
- [4] Neronov, A., Semikoz, D., submitted to *A&A* (preprint arXiv:1011.0210), 2010
- [5] Rousseau, R. et al., Observations of the PWN HESS J1857+026 with Fermi LAT, Fermi Symposium 2011, Rome
- [6] Paneque, D. et al., Sources in the Fermi Sky Above 10 GeV, Rome
- [7] Hinton, J., Hofmann, W., *Ann. Rev. Astron. Astrophys.*, 2009, **47**(523)
- [8] Klepser, S. et al., The MAGIC telescopes - Status and Recent Results, *Il Nuovo Cimento C*, 2011
- [9] Moralejo, A. et al., Proc. 31st ICRC (Łódź), 2009 (arXiv:0907.0943)
- [10] Carmona, E. et al., Performance of the MAGIC Stereo system, this conference, 2011
- [11] Albert, J. et al., *Nucl. Instr. Meth. A*, 2008, **588**(424)
- [12] Berger, K., Colin, P., Diago Ortega, A., Lombardi, S., Klepser, S. et al., Advanced stereoscopic gamma-ray shower analysis with the MAGIC telescopes, this conference, 2011
- [13] Albert, J. et al., *Nucl. Instr. Meth. A*, 2007, **583**(494)
- [14] Aharonian, F. et al., *A&A*, 2006, **460**(365)
- [15] Grondin, M.-H. et al., accepted for publication in *ApJ*, 2011 (preprint arXiv:1106.0184)